Enzymatic Activity of Lipase–Nanoparticle Conjugates and the Digestion of Lipid Liquid Crystalline Assemblies

ARTICLE *in* LANGMUIR · AUGUST 2010

Impact Factor: 4.46 · DOI: 10.1021/la1018604 · Source: PubMed

Langmuir Article

pubs.acs.org/Langmuir

Enzymatic Activity of Lipase−Nanoparticle Conjugates and the Digestion of Lipid Liquid Crystalline Assemblies

Jennifer L. Brennan,[†,#,◆] Antonios G. Kanaras,[Δ,◆] Paola Nativo,[†] T. Robert Tshikhudo,[†,○] Claire Rees,[†] Laura Cabo Fernandez,[†] Nijole Dirvianskyte,[§] Valdemaras Razumas,[§] Michael Skjøt,[‡] Allan Svendsen,[‡] Christian I. Jørgensen,[‡] Ralf Schweins,[∥] Malin Zackrisson,[⊥] Tommy Nylander,[⊥] Mathias Brust,*[,†] and Justas Barauskas*[,§,◆]

[†]*Liverpool Institute for Nanoscale Science Engineering and Technology, Department of Chemistry, University of Liverpool, Liverpool, L69 7ZD, U.K.,* [Δ]*School of Physics and Astronomy, University of Southampton, Highfield, Southampton, SO17 1BJ, U.K.,* [§]*Institute of Biochemistry, Mokslininku 12, LT-08662 Vilnius, Lithuania,* [‡]*Novozymes A/S, Smørmosevej 25, DK-2880, Bagsvaerd, Denmark,* [∥]*Institut Laue-Langevin, LSS group, 6 rue Jules Horowitz 38042 Grenoble Cedex 9, France, and* [⊥]*Physical Chemistry, Lund University, P.O. Box 124, SE-221 00 Lund, Sweden.* [#]*Present address: Irish Research Council for Science Engineering and Technology (IRCSET), Brooklawn House, Crampton Avenue, Dublin 4, Ireland.* [○]*Present address: Advanced Materials Division, Mintek, 200 Hans Strydom Drive, Randburg 2125, South Africa.* [◆]*These authors contributed equally in this project.*

Received May 10, 2010. Revised Manuscript Received June 29, 2010

Variants of lipase were attached to gold nanoparticles (NPs) and their enzymatic activity was studied. The two bioengineered lipase variants have been prepared with biotin groups attached to different residues on the protein outer surface. The biotinylation was evidenced by denaturing polyacrylamide gel electrophoresis and quantified by the ([2-(4′-hydroxyazobenzene)]benzoic acid spectrophotometric test. NPs of 14 ± 1 nm diameter coated with thiolated-polyethylene glycol ligands containing controlled proportions of biotin moieties have been prepared and characterized by transmission electron microscopy, UV−vis spectroscopy, small angle neutron scattering, and elemental analysis. These biotin-functionalized NPs were conjugated to lipase using streptavidin as a linker molecule. Enzyme activity assays on the lipase−nanoparticle conjugates show that the lipase loading and activity of the NPs can be controlled by varying the percentage of biotin groups in the particle protecting coat. The lipase−NP conjugates prepared using one variant display higher activity than those prepared using the other variant, demonstrating orientation-dependent enzyme activity. Cryogenic transmission electron microscopy was used to visualize the enzymatic activity of lipase−NP on well-defined lipid substrates. It was found that lipase-coated NPs are able to digest the substrates in a different manner in comparison to the free lipase.

Introduction

The chemistry of living cells is characterized by the simultaneous occurrence of a large number of processes, each of which may involve only relatively few molecules confined within a highly heterogeneous environment that is filled up with densely packed supramolecular structures. Examples of such systems are the multienzyme complex in the respiratory chain, where the proximity of the enzymes for the electron transfer processes is relatively well understood[1] and in the so-called cellulosome, which is an assembly of different cellulose degrading enzymes that is responsible for degradation of cellulose in nature.[2] Such natural systems point to the fact that the knowledge of equilibrium concentrations of metabolites and proteins in, for example, the cytosol, envisaged as a dilute aqueous solution, can be of limited value for the understanding of key biochemical processes which depend on spatially and temporally highly coordinated molecular interactions. Inspired by these enzyme assemblies in nature, the merging of bio and nanotechnology has generated a new and interesting class of functional assemblies with a host of applications in fields such as biosensors, drug delivery, medical diagnostics, tissue engineering, and molecular electronics.[3−7] The preparation of hybrid nanomaterials in which the inherent functionality of a biomolecule is controlled on the molecular level by a nonbiological component is an interesting concept that may lead to more efficient usage of biomolecules in applications at the interface of biology and technology.[8] A particular example is the development of imaging tools that are capable of localizing and identifying individual molecules inside the cell with the ultimate goal of obtaining a time and space resolved picture of every single molecule involved in a particular biochemical process, which might become feasible only in the more distant future. Outside the context of the living cell there is already a burgeoning interest in studies of single biomolecules which have been realized in various ways including, for example, the use of spectroscopic, X-ray, and neutron scattering and scanning probe and electron

*To whom correspondence should be addressed. (J.B.) Tel.: +370 52729068. Fax: +370 52729196. E-mail: justas.barauskas@bchi.lt. (M.B.) Tel.: +44 151 794 3554. Fax: +44 151 794 3588. E-mail: m.brust@liv.ac.uk.

(1) Nelson, D. L.; Cox, M. M. *Lehninger Principles of Biochemistry*, 4th ed.; W. H. Freeman and Company: New York, 2005.
(2) Bayer, E. A.; Kenig, R.; Lamed, R. *J. Bacteriol.* **1983**, *156*, 818–827.
(3) Pellegrino, T.; Kudera, S.; Liedl, T.; Munoz Havier, A.; Manna, L.; Parak, W. J. *Small* **2005**, *1*, 48–63.
(4) Rosi, N. L.; Mirkin, C. A. *Chem. Rev.* **2005**, *105*, 1547–1562.
(5) Alivisatos, A. P. *Nat. Biotechnol.* **2004**, *22*, 47–52.
(6) Kayser, O.; Lemke, A.; Hernandez-Trejo, N. *Curr. Pharm. Biotechnol.* **2005**, *6*, 3–5.
(7) Willner, I.; Katz, E. *Angew. Chem. Int. Ed.* **2004**, *43*, 6042–6108.
(8) Langer, R.; Tirrell, D. A. *Nature* **2004**, *428*, 487–492.

microscopy techniques.[9−18] In particular, recent advances in functionalizing nanoparticles with complex macromolecules[19,20] provide completely new opportunities of single molecule tagging and tracing.

The most significant previous research in this area has focused on bioconjugates between DNA and gold nanoparticles, prepared using well-established gold−thiol chemistry.[21−27] These new materials have inspired important developments both in nanotechnology and bioanalytical sciences owing to both the unique structural and molecular recognition properties of DNA and the highly sensitive optical properties of NPs. Bioconjugates of proteins (e.g., enzymes, antibodies) and NPs have been created using a range of binding methods, such as electrostatic, covalent, or specific affinity methods. With a few exceptions,[28,29] the attachment of enzymes to NPs has mainly relied on noncovalent electrostatic or hydrophobic interactions.[30,31] The usefulness of such conjugates for the aforementioned applications could be limited due to the possibility of the proteins detaching from the nanoparticle surface. An attractive alternative is to conjugate proteins and enzymes and NPs via the strong specific (but noncovalent) interaction between biotin and avidin (or streptavidin).[32−35] Such control of enzymatic activity is of significance in therapeutics and pharmaceutics where it could assist in developing methods for the treatment and prevention of numerous human diseases and disorders.[36−39]

Lipase-catalyzed lipolyses is of paramount physiological importance.[40] In addition lipase-catalyzed lipolyses has come to large industrial importance in many technical applications, including detergency and food processing.[41] The natural lipids have low aqueous solubility and therefore form various self-assembled structures that strongly depend on the lipid composition. Lipolyses catalyzed by the water-soluble lipase therefore takes place at the aqueous−lipid interface and is extremely dependent on the structure and organization of the lipid/water boundary.[42] During the reaction hydrolysis products interact with lipids, continuously change the interface characteristics, and alter cleavage mechanisms from the complex lipid aggregate. It can be shown that the phase diagram of the substrate/product can be used to predict the evolution of the self-assembly system.[43,44] Lipase molecules act at such a low concentration that their presence as protein does not significantly affect the global lipid self-assembly structure. Rather, it is their catalytic activity that has an impact on the lipid self-assembly structure. The challenge is to understand the self-assembly structural changes on the nanoscale level and thereby the enzymatic action on the single molecule level. This can be achieved for a supported bilayer by using atomic force microscopy (AFM) on the 2D system.[45,46]

In this study, biotin and streptavidin have been utilized to link biotinylated lipase molecules to biotinylated NPs using streptavidin as "molecular glue" (Scheme 1). A lipase (from *Thermomyces lanuginosus*) has been modified to contain lysine residues only at specific locations within the protein structure, allowing them to be biotinylated only at these locations, which in turn permits control over their orientation when attached to the nanoparticle surface. Here we show that this can alter the enzyme's activity by selecting appropriate lipase variants for the construction of enzyme−NP conjugates. Furthermore, we demonstrate that enzymatic activity of lipase−NP conjugates can be monitored at the level of single active units by cryogenic transmission electron microscopy (cryo-TEM) on the 3D lipid liquid crystalline aggregates. Here the gold nanoparticles act as an electron-dense contrast agent for cryo-TEM and allow the visualization of not only the lipid aggregates but also the enzyme. We have studied the enzymatic digestion of lipids within glycerol monooleate (GMO)-based nanoscale liquid crystalline assemblies, so-called cubosomes,[47] that consist of colloidal 50−500 nm particles with a distinctive internal cubic liquid crystalline nanostructure, low degree of polydispersity, and long-term stability.[48,49] We show that upon enzyme-induced hydrolysis of their constituent lipids, the cubosomes transform into other self-assembled aggregates that can be easily monitored by cryo-TEM.

(9) Strozecka, A.; Myslivecek, J.; Voigtlander, B. *Appl. Phys. A: Mater. Sci. Process.* **2007**, *87*, 475–478.
(10) Fron, E.; Flors, C.; Schweitzer, G.; Habuchi, S.; Mizuno, H.; Ando, R.; De Schryver, F. C.; Miyawaki, A.; Hofkens, J. *J. Am. Chem. Soc.* **2007**, *129*, 4870–4871.
(11) Reinhard, B. M.; Sheikholeslami, S.; Mastroianni, A.; Alivisatos, A. P.; Liphardt, J. *Proc. Natl. Acad. Sci. U.S.A.* **2007**, *104*, 2667–2672.
(12) Malac, M.; Beleggia, M.; Egerton, R.; Zhu, Y. M. *Ultramicroscopy* **2007**, *107*, 40–49.
(13) Van Zalinge, H.; Schiffrin, D. J.; Bates, A. D.; Haiss, W.; Ulstrup, J.; Nichols, R. J. *ChemPhysChem* **2006**, *7*, 94–98.
(14) Flomenbom, O.; Hofkens, J.; Velonia, K.; De Schryver, F. C.; Rowan, A. E.; Nolte, R. J. M.; Klafter, J.; Silbey, R. J. *Chem. Phys. Lett.* **2006**, *432*, 371–374.
(15) Kufer, S. K.; Dietz, H.; Albrecht, C.; Blank, K.; Kardinal, A.; Rief, M.; Gaub, H. E. *Eur. Biophys. J.* **2005**, *35*, 72–78.
(16) Velonia, K.; Flomenbom, O.; Loos, D.; Masuo, S.; Cotlet, M.; Engelborghs, Y.; Hofkens, J.; Rowan, A. E.; Klafter, J.; Nolte, R. J. M.; De Schryver, F. C. *Angew. Chem., Int. Ed.* **2005**, *44*, 560–564.
(17) Sonnichsen, C.; Reinhard, B. M.; Liphardt, J.; Alivisatos, A. P. *Nat. Biotechnol.* **2005**, *23*, 741–745.
(18) Flomenbom, O.; Velonia, K.; Loos, D.; Masuo, S.; Cotlet, M.; Engelborghs, Y.; Hofkens, J.; Rowan, A. E.; Nolte, R. J. M.; Van der Auweraer, M.; De Schryver, F. C.; Klafter, J. *Proc. Natl. Acad. Sci. U.S.A.* **2005**, *102*, 2368–2372.
(19) Tshikhudo, T. R.; Demuru, D.; Wang, Z. X.; Brust, M.; Secchi, A.; Arduini, A.; Pochini, A. *Angew. Chem., Int. Ed.* **2005**, *44*, 2913–2916.
(20) You, C. C.; Chompoosor, A.; Rotello, V. M. *Nanotoday* **2007**, *2*, 34–43.
(21) Mirkin, C. A.; Letsinger, R. L.; Music, R. C.; Storhoff, J. J. *Nature* **1996**, *382*, 607–609.
(22) Alivisatos, A. P.; Johnsson, K. P.; Peng, X. G.; Wilson, T. E.; Loweth, C. J.; Bruchez, M. P.; Schultz, P. G. *Nature* **1996**, *382*, 609–611.
(23) Niemeyer, C. M.; Ceyhan, B.; Hazarika, P. *Angew. Chem., Int. Ed.* **2003**, *42*, 5766–5770.
(24) Kanaras, A. G.; Wang, Z.; Bates, A. D.; Cosstick, R.; Brust, M. *Angew. Chem., Int. Ed.* **2003**, *42*, 191–194.
(25) Wang, Z.; Kanaras, A. G.; Bates, A. D.; Cosstick, R.; Brust, M. *J. Mater. Chem.* **2004**, *14*, 578–580.
(26) Kanaras, A. G.; Wang, Z.; Brust, M.; Cosstick, R.; Bates, A. D. *Small* **2007**, *3*, 590–594.
(27) Kanaras, A. G.; Wang, Z.; Hussain, I.; Brust, M.; Cosstick, R.; Bates, A. D. *Small* **2007**, *3*, 67–70.
(28) Abad, J. M.; Mertens, S. F. L.; Pita, M.; Fernandez, V. M.; Schiffrin, D. J. *J. Am. Chem. Soc.* **2005**, *127*, 5689–5694.
(29) Simonian, A. L.; Good, T. A.; Wang, S.-S.; Wild, J. R. *Anal. Chim. Acta* **2005**, *534*, 69–77.
(30) Ha, T. H.; Jeong, J. Y.; Chung, B. H. *Chem. Commun.* **2005**, *48*, 3959–3961.
(31) You, C.-C.; Agasti, S. S.; De, M.; Knapp, M. J.; Rotello, V. M. *J. Am. Chem. Soc.* **2006**, *128*, 14612–14618.
(32) Schroedter, A.; Weller, H. *Angew. Chem., Int. Ed.* **2002**, *41*, 3218–3221.
(33) Wang, Z.; Lee, J.; Cossins, A. R.; Brust, M. *Anal. Chem.* **2005**, *77*, 5770–5774.
(34) Wang, Z.; Levy, R.; Fernig, D. G.; Brust, M. *J. Am. Chem. Soc.* **2006**, *128*, 2214–2215.
(35) Aslan, K.; Luhrs, C. C.; Perez-Luna, V. H. *J. Phys. Chem. B* **2004**, *108*, 15631–15639.
(36) Leung, D.; Abbenante, G.; Fairlie, D. P. *J. Med. Chem.* **2000**, *43*, 305–341.
(37) Aguiar, M.; Masse, R.; Gibbs, B. F. *Drug Metab. Rev.* **2005**, *37*, 379–404.
(38) Belinsky, S. A.; Nikula, K. J.; Baylin, S. B.; Issa, J. P. J. *Proc. Nat. Acad. Sci. U.S.A.* **1996**, *93*, 4045–4050.
(39) Esler, W. P.; Wolfe, M. S. *Science* **2001**, *293*, 1449–1454.
(40) Patton, J. S.; Carey, M. C. *Science* **1979**, *204*, 145–148.
(41) Svendsen, A. *Biochim. Biophys. Acta* **2000**, *1543*, 223–238.
(42) Verger, R. *Trends Biotechnol.* **1997**, *15*, 32–38.
(43) Borné, J.; Nylander, T.; Khan, A. *Langmuir* **2002**, *18*, 8972–8981.
(44) Borné, J.; Nylander, T.; Khan, A. *J. Phys. Chem. B* **2002**, *106*, 10492–10500.
(45) Balashev, K.; Gudmand, M.; Iversen, L.; Callisen, T. H.; Svendsen, A.; Bjørnholm, T. *Biochim. Biophys. Acta, Biomembr.* **2003**, *1615*, 93–102.
(46) Balashev, K.; Dinardo, J.; Callisen, T.; Svendsen, A.; Björnholm, T. *Biochim. Biophys. Acta, Biomembr.* **2007**, *1768*, 90–99.
(47) Cubosome is a UPSTO registered trademark of Camurus AB, Sweden.
(48) Barauskas, J.; Johnsson, M.; Joabsson, F.; Tiberg, F. *Langmuir* **2005**, *21*, 2569–2577.
(49) Barauskas, J.; Johnsson, M.; Tiberg, F. *Nano Lett.* **2005**, *5*, 1615–1619.

Scheme 1. Cartoon Depicting Biotin−Streptavidin−Biotin Conjugation Method

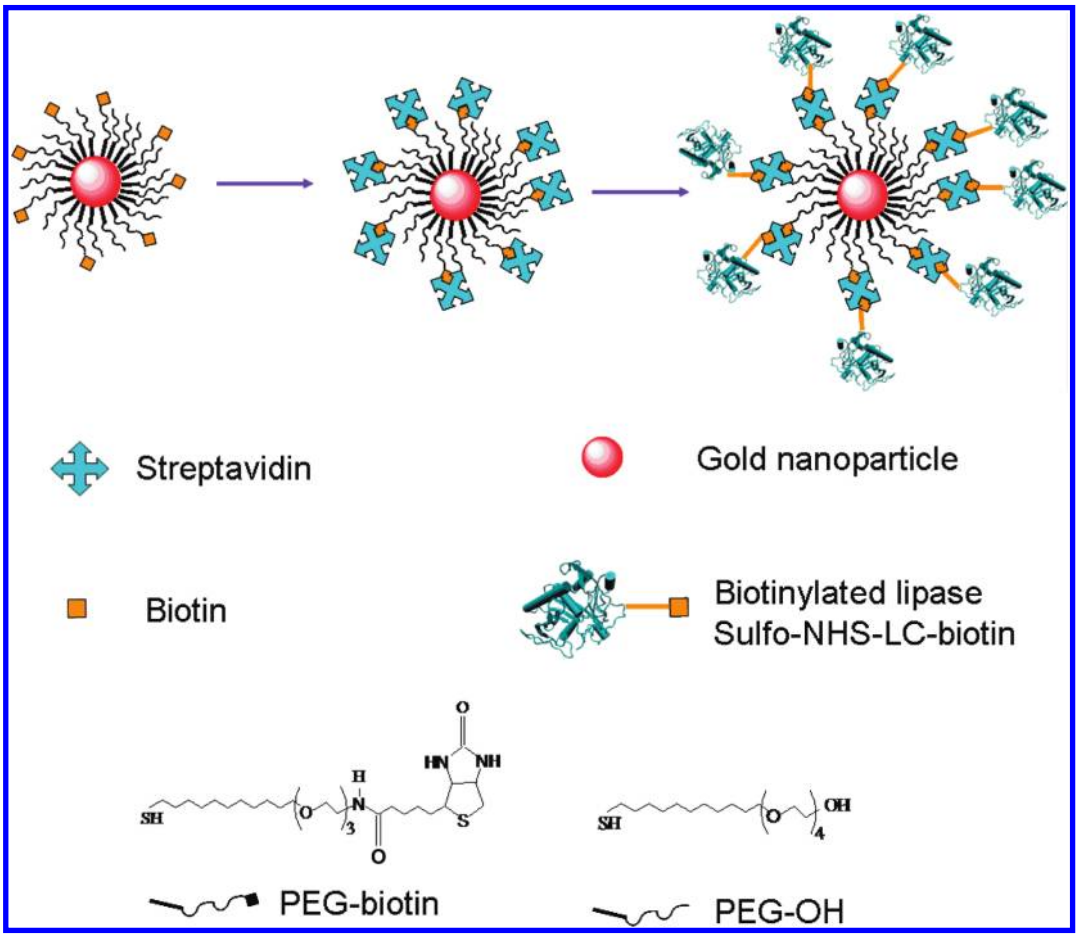

Materials and Methods

Lipids. Thioalkylated PEG−biotin (5-(2-oxo-hexahydro-thieno-[3,4-d]imidazol-4-yl)-pentanoic acid (2-{2-[2-(11-mercapto-undecycloxy)-ethoxy]-ethoxy}-ethyl)-amide; PEG−biotin) and monohydroxy (1-mercaptoundec-11-yl) tetraethyleneglycol (PEG−OH) were purchased from Prochimica (Poland). RYLO MG 19 glycerol monooleate (GMO) (96.7% monoglycerides) was produced and provided by Danisco Ingredients (Brabrand, Denmark) with the following fatty acid composition (lot no. 2119/65-1): 89.3% oleic, 4.6% linoleic, 3.4% stearic, and 2.8% palmitic acid. The poly(ethylene oxide) (PEO)-poly(propylene oxide) (PPO)-poly-(ethylene oxide) triblock copolymer with the trade name Pluronic F127 and approximate formula of $PEO_{98}PPO_{57}PEO_{98}$ (average molecular weight of 12600 g/mol) was obtained from BASF Svenska AB (Helsingborg, Sweden). Unless otherwise stated, all other chemicals were obtained from Sigma Aldrich Company Ltd. and were used as received. Milli-Q water (18.2 MΩ), purified with an ultrapure water system Milli-Q Plus 185 (Millipore purification pack), was used throughout

Lipase Variants. Variants of the *Thermomyces lanuginosus* (previously *Humicola lanuginosus*) lipase (E.C.3.1.1.3) were generated and purified as described previously.[50] Two variants were prepared. L1 was engineered to K24R, N33Q, K74R, K98R, K127R, R175K, K223R, K237R, whereas L2 was mutated to K24R, N33Q, K46R, K74R, K98R, K127R, D137K, K223R, K237R. This mutation code uses the standard single letter amino acid code and should be interpreted as follows: for example, K24R indicates that a lysine at position 24 has been mutated to arginine. The full mutation code for the variants indicates that they were modified to contain either one or two lysine residues on the protein surface, L2 at pos. 137 and L1 at pos. 46 and 175, respectively. The lipase variants L1 and L2 were engineered to contain specific solvent-accessible lysine NH_2 groups. They were labeled with a biotin group using the biotinylation reagent EZ-Link Sulfo-NHS-LC-Biotin (sulfosuccinimidyl-6-(biotinamido)-hexanoate, Pierce). The reaction was carried out in 0.1 mM phosphate buffer, 0.15 M sodium chloride, pH 7.2 (PBS). A 1700 μL portion of lipase solution (0.057 mM in PBS) and 144 μL of EZ-Link Sulfo-NHS-LC-Biotin solution (100 mM in H2O) were mixed in a 1.5 mL microfuge tube. The reaction mixture was shaken for 6 h at room temperature. Reaction byproducts were removed by passing the mixture through a NAP-10TM disposable prepacked desalting column (Amersham Biosciences), equilibrated with phosphate-buffered saline (PBS). To ensure complete removal of excess biotinylation reagent, the remaining mixture was dialyzed three times against 500 mL of PBS for a total of 36 h using a molecular weight cutoff of 12 kDa.

To quantify biotin label incorporation, a spectrophotometric test using HABA ([2-(4′-hydroxyazobenzene)]benzoic acid, Pierce) was utilized, in which a solution containing the biotinylated enzyme was added to a mixture of HABA and avidin.[51] Because of its higher affinity for avidin, the biotin on the enzyme displaces the HABA from its interaction with avidin, and the measured visible absorption at 500 nm decreases. A stock solution of 10 mM HABA in 10 mM NaOH is prepared. A HABA−avidin solution is prepared by adding 600 μL of HABA stock to 10 mg of avidin dissolved in 19.4 mL of PBS. The absorbance at 500 nm of 180 μL of HABA−avidin solution is measured, 20 μL of biotinylated protein is added, and the absorbance remeasured 1 min after

(50) Svendsen, A.; Clausen, I. G.; Patkar, S. A.; Borch, K.; Thellersen, M. *Methods Enzymol.* **1997**, *284*, 317–340.

(51) Janolino, V. G.; Fontecha, J.; Swaisgood, H. E. *Appl. Biochem. Biotechnol.* **1996**, *56*, 1–7.

thorough mixing. The measured change in absorbance after addition of biotinylated enzyme is used to calculate the number of moles of biotin per mole of protein.

To electrophoretically demonstrate the successful biotinylation of the enzyme, samples of the biotin-labeled and unlabeled enzyme were analyzed using SDS-PAGE (sodium dodecyl sulfate polyacrylamide gel electrophoresis, 15%). The gels were prepared and run using a BioRad Mini-PROTEAN 3 system, and were postrun stained using EZBlue Gel Staining Reagent. Samples were run alongside BioRad Precision Plus protein dual-color molecular weight standards. The lipase activity of the biotinylated enzyme was confirmed using a lipase activity assay (described below).

Preparation of Modified Gold Nanoparticles. Citrate-stabilized NPs of 14 ± 1 nm diameter were synthesized using the classical Turkevich/Frens procedure.[52,53] Briefly, an aqueous solution of sodium citrate (25 mL, 39 mM) was added to a boiling aqueous solution of $HAuCl_4$ (250 mL, 1 mM), and the reaction mixture was heated under reflux for 30 min. It was allowed to cool to room temperature, stirred overnight, and filtered before use through a 0.45 μm syringe filter (Millipore).

NPs coated with a mixture of 1% PEG−biotin and 99% PEG−OH (1%B−Au), were prepared as previously reported.[54] Briefly, 77 μL of a methanolic solution of PEG−OH, monohydroxy (1-mercaptoundec-11yl) tetraethylene glycol (MW: 380), (4.89 mg, 1.3×10^{-2} mmol) and 3.5 μL of a methanolic solution of thioalkylated, biotin (1-mercaptoundec-11yl) triethylene glycol (MW: 561), PEG−biotin (0.073 mg, 1.3×10^{-4} mmol) were mixed and added to filtered citrate-stabilized gold NP (20 mL, 2 nM). The reaction mixture was stirred at room temperature overnight and then purified by repeated centrifugation and redispersion (three times, at 10000*g*) in 20 mM phosphate buffer, pH 7.4. The particles were further purified by size-exclusion chromatography (15 × 1 cm, Sephacryl 100 HR) and stored in 20 mM phosphate buffer, pH 7.4. A molar extinction coefficient of 2.89×10^8 M^{-1} cm^{-1} (at 522 nm) based on gold NPs of 14 ± 2 nm diameter was used to calculate the nanoparticle concentration.[55,56] To prepare NPs functionalized with 10% PEG−biotin and 90% PEG−OH (10%B−Au), the protocol described above was followed except that in this case 70 μL of a methanolic solution of PEG−OH (4.45 mg, 1.3×10^{-2} mmol) and 35 μL of a methanolic solution of PEG−biotin (0.73 mg, 1.3×10^{-3} mmol) were mixed and added to the citrate gold NP (20 mL, 2 nM). Purification was identical to that carried out for 1%B−Au. The nanoparticle diameter was verified by transmission electron microscopy (TEM) using a JEOL 2000 EX transmission electron microscope operating at 200 kV. Specimens for TEM were prepared by the slow evaporation of one drop of an aqueous solution of the NPs onto a carbon-coated copper mesh grid. ICP-AES (inductively coupled plasma atomic emission spectroscopy) of an aqua regia-digested dried nanoparticle pellet yielded experimental gold and sulfur contents of 284.2 and 1.55 ppm, respectively. The average number of capping ligands per NP for both particle types can be estimated as 2880 ± 130 from this gold and sulfur content, assuming an average number on the order of 85000 gold atoms per particle.[57]

To coat these biotinylated NPs with streptavidin, a solution of NPs was mixed with a 50-fold molar excess of streptavidin in PBS and incubated overnight at 4 °C, after which the NPs were purified by repeated centrifugation (six times at 10000*g*) and redispersion in PBS. These streptavidin-coated NPs were incubated overnight at 4 °C with a 20-fold molar excess of biotinylated enzyme and purified by centrifugation/redispersion as before. The supernatants were retained and tested for the presence of lipase using a lipase activity assay (described below).

Dot-Blot was utilized to detect available biotin or streptavidin on the gold NPs. Drops of NP solutions of varying concentration were immobilized as individual spots on a 0.45 μm pore size PVDF membrane, and the membrane was incubated with a blocking agent (Bovine Serum Albumin (BSA)/PBS - 25 μL, 5 mg/mL) for 40 min in order to prevent nonspecific protein interactions. To detect available biotin, the membrane was incubated for 30 min with a solution of StrepTactin−horseradish peroxidase (HRP) (2 μL) with BSA/PBS (15 mL, 5 mg/mL) and Tween 20 (75 μL, 100%), then washed 5 times with PBS/Tween 20 (15 mL, 0.5%) and twice with PBS and water respectively. Chemiluminescence detection was carried out following 5 min incubation with luminol (400 μL) and hydrogen peroxide (400 μL). The emission of light was detected on a photographic film. To detect available streptavidin, a similar protocol was used but with Biotin-HRP instead of StrepTactin-HRP.

Estimating Number of Lipase Molecules per Particle. An amino acid assay was used to determine an average number of lipase molecules per lipase−nanoparticle conjugate. Bionanoconjugates were hydrolyzed in 18.5% HCl + 0.1% phenol and incubated at 110 °C for 16 h. The mixture was dried and resolved in loading buffer (0.2 M sodium citrate, pH 2.2), filtrated, and loaded onto a Biochrom 20 Plus amino acid analyzer. The determined amino acid content was fitted to the protein theoretical amino acid composition, and the experimental amount was calculated. Concentration of enzyme-coated nanoparticles: 145 nM of nanoparticles or 29 pmol of nanoparticles per 200 μL of solution. Two independent measurements were carried out. Sample 1: 0.015 mg/mL total amount of protein or 100 pmol of total protein. Sample 2: 0.035 mg/mL total amount of protein or 233 pmol of total protein. If the relation of streptavidin lipase is 1:1 (consider dot blot experimental results) then the lipase amount per particle will be 1−2 enzyme molecules per particle for sample 1 and 2−4 enzyme molecules per particle for sample 2.

Determining the Properties of Modified Gold Nanoparticles. Small angle neutron scattering (SANS) experiments were performed at the large scale structure diffractometer D22 at the Institut Laue Langevin (Grenoble, France). Three configurations were used with sample-to-detector distances (1.5, 8.0, and 17.6 m) together with three collimation lengths (4.0, 8.0, and 17.6 m) resulting in a q range, $0.0010 < q < 0.2285$ Å^{-1}. A detector offset of 400 mm, a wavelength of 16 Å, and circular quartz cuvettes from Helma (1 or 2 mm optical path length) were used in all measurements. Two-dimensional spectra were azimuthally averaged using standard ILL software. After background subtraction, correction for empty cell, and transmissions, absolute intensities were determined by using water as a standard. Experimentally obtained SANS data suffer from smearing due to the instrumental setup which smoothes sharp features in the measured intensity. This smearing needs to be corrected for. The analytical expressions given by Pedersen et al.[58] and Barker and Pedersen[59] are used here. We note the finite collimation effect on the resolution of the scalar q vector originates from work by Mildner and Carpenter.[60] As input to the smearing algorithm collimation distances, detector resolution (full-width at half-maximum) is 0.8 cm, detector annulus width is 1 cm, $\Delta\lambda/\lambda$ is 0.10, source aperture dimensions is 5.0 cm, and sample aperture dimensions are 1.6 cm. The scattered intensity is fitted to a form factor assuming that the structure factor is equal to 1 and that interactions are negligible since the highest measured concentration in these experiments is 100 mM Au, which corresponds to a Au particle weight fraction of 0.2 wt % for the PEG, biotin, and streptavidin particles.

(52) Turkevich, J.; Stevenson, P. C.; Hillier, J. *Discuss. Faraday Soc.* **1951**, *11*, 55–57.
(53) Frens, G. *Nat. Phys. Sci.* **1973**, *241*, 20–22.
(54) Tshikhudo, T. R.; Demuru, D.; Wang, Z.; Brust, M.; Secchi, A.; Arduini, A.; Pochini, A. *Angew. Chem., Int. Ed.* **2005**, *44*, 2913–2916.
(55) Link, S.; Wang, Z. L.; El-Sayed, M. A. *J. Phys. Chem. B* **1999**, *103*, 3529–3533.
(56) Mulvaney, P.; Giersig, M.; Henglein, A. *J. Phys. Chem.* **1992**, *96*, 10419–10424.
(57) Yang, W.; Chen, M.; Knoll, W.; Deng, H. *Langmuir* **2002**, *18*, 4124–4130.
(58) Pedersen, J. S.; Posselt, D.; Mortensen, K. *J. Appl. Crystallogr.* **1990**, *23*, 321–333.
(59) Barker, J. G.; Pedersen, J. S. *J. Appl. Crystallogr.* **1995**, *28*, 105–114.
(60) Mildner, D. F. R.; Carpenter, J. M. *J. Appl. Crystallogr.* **1984**, *17*, 249–256.

The concentration of lipase particles was even lower (0.02 wt %). To correct for anomalites in the scattering pattern in the treatment of data, individual masks were created for each diffractogram.

In small-angle neutron scattering experiments the coherent differential scattering cross-section $I(q)$ is measured as a function of the magnitude of the scattering vector q, defined as $q = (4\pi/\lambda) \cdot \sin(\theta/2)$, where λ is the neutron wavelength and θ is the scattering angle. For a dilute system of polydisperse noninteracting particles $I(q)$ takes the form

$$I(q) = \frac{N}{V}(\rho_s - \rho_p)^2 \int_0^\infty f(r)\, A(q,r)\, A(q,r)^*\, dr$$

where N/V is the number density of particles and ρ_s and ρ_p are the scattering length density of the solvent and particles, respectively. $A(q)$ is the form amplitude and defines the form factor simply as $P(q) = |A(q)|^2$. Particle polydispersity is taken into account by integrating over a size distribution $f(r)$. We make use of the analytical form factor for core−shell spherical particles with a Schultz distribution derived by Hayter.[61] In the model R_0 is the outer radius and R_i is the inner core radius, and the shell thickness d is defined as $R_0 - R_i$. Polydispersity is defined as $\sigma/\langle R_0 \rangle$, with σ being the standard deviation.

Assay of Lipase Activity. Lipase activity was determined using a fluorescence-based activity assay adapted from that reported by Guilbault and Hieserman.[62] A nonfluorescent substrate, 5-*O*-palmitoylindole was employed.[63] In the presence of lipase, the palmitoyl chain of the substrate is cleaved at the ester bond, yielding a fluorescent 5-OH-indole product. Briefly, 30 μL of 5-*O*-palmitoylindole in 2-methoxyethanol was mixed with 70 μL of PB, and 20 μL of lipase (or nanoparticle) sample was added, while a stop clock was started simultaneously. The emission intensity of the assay mixture at the start and end of 5 min incubation was monitored using a Perkin-Elmer LS50B luminescence spectrometer (λ_{ex} = 300 nm, λ_{em} = 333 nm). The rate of change of emission intensity with respect to time (min^{-1}) is converted to enzyme activity units (U mL^{-1}) using the molar fluorescence of 5-OH-indole (1.15×10^9 mL mol^{-1} in this assay). One activity unit (U) is equivalent to 1 micromole of 5-OH-indole product liberated per minute. The blank rate of the assay (autohydrolysis of the substrate) was determined by substituting 20 μL of PB for the 20 μL of lipase sample in the assay mixture. This control experiment demonstrated that autohydrolysis of the substrate was negligible under these assay conditions. As NPs absorb strongly at both the excitation and emission wavelength of 5-OH-indole, it is likely that the fluorescence quantum yield of the 5-OH-indole fluorophore will be lower when NPs are present in the lipase assay solution. To quantify this "quenching" effect, a Stern−Volmer-type quenching constant, K_{SV}, for the gold NPs and 5-OH-indole was determined to be 5.57×10^7 M^{-1} for this system. All quoted nanoparticle−lipase activity rates have been corrected using this K_{SV}. The activity is expressed as "activity per nM of NP−conjugate", where the molar concentration of NPs in the sample is determined by UV−vis with $\varepsilon = 2.89 \times 10^8$ M^{-1} cm^{-1},[55,56] assuming that lipase activity is neither increased nor decreased upon binding to the nanoparticle.

Preparation of Lipid-Based Liquid Crystalline Particles. Dispersed submicrometer-size lipid liquid crystalline particles were prepared by adding appropriate amounts of melted GMO into an aqueous F127 solution. In all experiments the lipid/polymer ratio was 9/1 (w/w) and the total amphiphile (lipid + polymer) concentration was 2 wt %. The sample volume was usually 50−100 mL. The samples were immediately sealed, hand-shaken, and mixed for 24−48 h on a mechanical mixing rocking table at 350 rpm and room temperature. The resulting coarse dispersions were homogenized by passing the mixture 5−8 times through a Microfluidizer 110S (Microfluidics Corp., Newton, MA) at 345 bar and 25 °C. To prepare nanoparticles with a high degree of order, low polydispersity, and low contamination of metastable vesicular aggregates, homogenized dispersions were subjected to heat treatment procedure. Heat treatment of the dispersions was performed using a bench-type autoclave (CertoClav CV-EL, Certoclav Sterilizer GmbH, Traun, Austria) operated at 125 °C and 1.4 bar. The samples were filled into Pyrex glass bottles (100−200 mL) and put into the autoclave. A period of about 12 min was required to vent the entrapped air and to heat up the autoclave. The samples were then subjected to heat treatment for 20 min at 125 °C. After the heat treatment, the samples were allowed to cool to room temperature before experiments.

Cryogenic Transmission Electron Microscopy (cryo-TEM) for Nanoscale Imaging. The samples for cryogenic transmission electron microscopy (cryo-TEM) were prepared in a controlled environment vitrification system. The climate chamber temperature was 25−28 °C, and the relative humidity was kept close to saturation to prevent evaporation from the sample during preparation. A 5 μL sample drop was placed on a carbon-coated holey film supported by a copper grid and gently blotted with filter paper to obtain a thin liquid film (20−400 nm) on the grid. The grid was then rapidly plunged into a liquid ethane at −180 °C and transferred into liquid nitrogen (−196 °C). The vitrified specimens were stored in liquid nitrogen and transferred into a Philips CM120 BioTWIN microscope equipped with a postcolumn energy filter (Gatan GIF 100) using an Oxford CT 3500 cryo-holder and its workstation. The acceleration voltage was 120 kV and the working temperature was kept below −182 °C. The images were recorded digitally with a CCD camera (Gatan MSC 791) under low-dose conditions with an underfocus of approximately 1 μm.

Results and Discussion

Lipase Biotinylation. The enzymes studied here are variants of a lipase (TLL) from the fungus *Thermomyces lanuginosus*. This is a commercially relevant enzyme used widely within the detergent, paper, food, and chemical industries.[64,65] A collective structure of the lipase variants used in this study is shown in Figure 1. The active site of the enzyme is contained within a cavity capped by a "lid", which remains tightly closed in pure aqueous solution, preventing access to the active site.[66] When a hydrophobic material, such as a lipid chain is introduced to the system, the lid opens and access to the active site is granted.[67] The two variants used here differ in the position of their lysine residues, with L1 having two: one inside the cavity containing the active site's catalytic triad of amino acids, and one on the protein's outer surface, relatively near to the lid and active site. L2's single lysine is situated on the protein's outer surface, on the opposite side to the lid and active site.

Both variants were biotin-labeled using a water-soluble commercial biotinylation reagent, Sulfo-NHS-LC-biotin, which contains an active sulfo-*N*-hydroxysuccinamide (sulfo-NHS) ester for rapid and facile coupling to lysine residues at pH 7, through the creation of a stable amide bond. Following purification, the percentage of biotin label incorporated into the lipase was determined using the colorimetric HABA test. HABA is a small dye which reacts strongly with avidin, leading to a strong absorbance band at 500 nm. When a biotin-containing molecule

(61) Hayter, J. P. In *Physics of Amphiphiles: Micelles, Vesicles, and Microemulsions*; Degiorgio, V., Corti, M., Eds.; Elsevier: Amsterdam, 1985; p 59.
(62) Guilbault, G. G.; Hieserman, J. *Anal. Chem.* **1969**, *41*, 2006–2009.
(63) Brennan, J. L.; Hatzakis, N. S.; Tskikhudo, T. R.; Dirvianskyte, N.; Razumas, V.; Patkar, S.; Vind, J.; Svendsen, A.; Nolte, R. J. M.; Rowan, A. E; Brust, M. *Bioconjugate Chem.* **2006**, *17*, 1373–1375.
(64) Svendsen, A. *Biochim. Biophys. Acta* **2000**, *1543*, 223–238.
(65) Valincius, G.; Ignatjev, I.; Niaura, G.; Kazemekaite, M.; Talaikyte, Z.; Razumas, V; Svendsen, A. *Anal. Chem.* **2005**, *77*, 2632–2636.
(66) Brzozowski, A. M.; Savage, H.; Verma, C. S.; Lawson, J. P. D. M.; Svendsen, A.; Patkar, S. A. *Biochemistry* **2000**, *39*, 15071–15082.
(67) Martinelle, M.; Holmquist, M.; Hult, K. *Biochim. Biophys. Acta* **1995**, *1258*, 272–276.

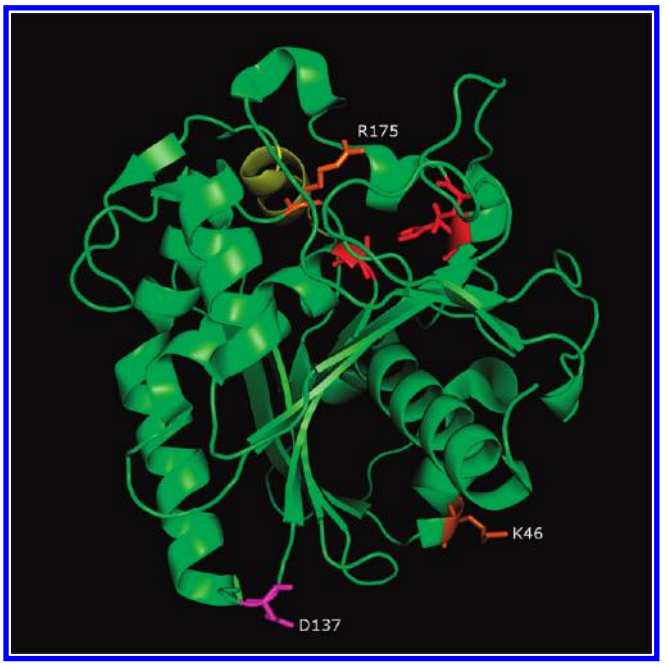

Figure 1. Collective structure of variants of *T. lanuginosus* lipase used in this study. Pertinent areas of the lipase structure are highlighted as follows: lid = yellow, red = catalytic triad of active site, orange = positions in L1 where a lysine residue was kept (K46) and a new lysine was introduced (R175K), and magenta = position in L2 where a lysine residue was introduced (D137K).

is added to a mixture of HABA and avidin, the biotin displaces the HABA from its interaction with avidin, causing a decrease in the measured absorbance, which is used to quantify the amount of biotin-labeling. For L1, the HABA test reveals a labeling yield of 82%. As the enzyme's lid remains tightly closed in the absence of organic solvents, the purely aqueous coupling conditions utilized here would prevent the labeling of the lysine residue inside the cavity. Therefore, this 82% refers to the labeling of the surface lysine and possibly the N-terminal amine of the protein. L2 yields a labeling efficiency of 137%, leading to the conclusion that some of the lipases have been biotinylated twice (through the N-terminal amine of the protein) leading to a sample containing a mixture of single- and double-labeled lipases.

The HABA test results were confirmed by sodium dodecylsulphate polyacrylamide gel electrophoresis (SDS-PAGE) under reducing conditions. The gels are shown in Figure 2, clearly demonstrating a difference in mobility between unlabeled (lane 2) and biotin-labeled (lane 3) lipase. The gel for L1 shows 1 band for the labeled lipase, indicating that merely 1 biotin group per lipase has been incorporated for this variant. The gel for L2 shows two bands for the labeled lipase, likely to be singly and doubly labeled lipase, as discussed earlier. However, the low intensity of the doubly labeled (upper) band suggests that the majority of the lipases in the sample are singly biotinylated.

To investigate whether incorporation of the biotin label has affected the enzymatic activity, a lipase assay was performed on the unlabeled and biotin-labeled variants. The assay is based on monitoring the rate of increase of fluorescence emission of the 5-OH-indole product liberated when a lipase cuts the ester bond in the 5-O-palmitoylindole assay substrate. The results demonstrate that biotin-L1 has 58% of the activity of unlabeled L1, while

(68) Deutscher, M. P. In *Methods in Enzymology*; Deutscher, M. P., Ed.; Academic Press: San Diego, 1990; Vol. *182*, p 83−89.

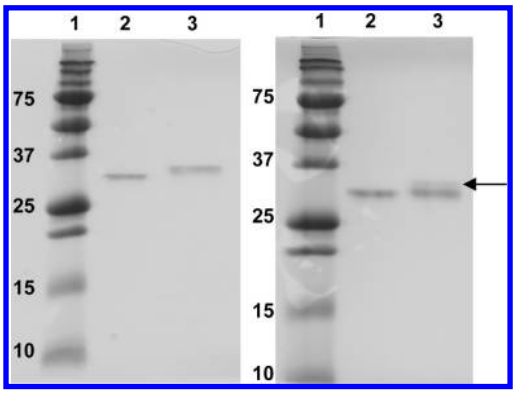

Figure 2. SDS-PAGE gels for biotinylated lipase variants. LHS = L1, RHS = L2. In both gels, lane 1 = molecular weight markers, lane 2 = unlabeled lipase, lane 3 = biotin labeled lipase.

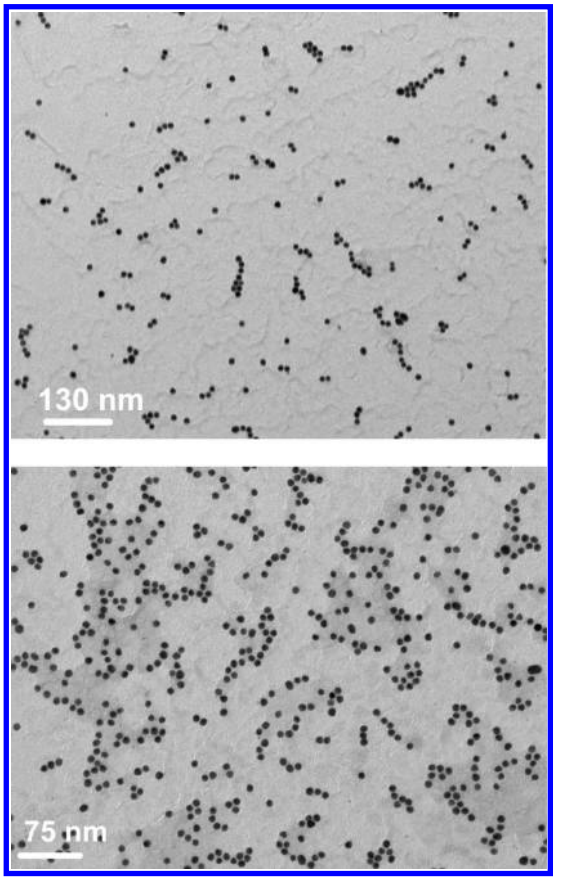

Figure 3. TEM images: SA-1%B−Au (top), and L1-SA-1% B−Au (bottom).

biotin-L2 has 62%. Such activity decreases are commonly observed following enzyme labeling and purification procedures.[68]

Preparation of Biotin-Functionalized Gold Nanoparticles. Biotin-functionalized NPs (1%B−Au and 10%B−Au) have been prepared by incubating citrate-stabilized gold NPs with a methanol/water mixture of the water-soluble thioalkylated oligo(ethylene glycol) ligands, PEG−OH and PEG−biotin. Following purification by centrifugation and gel filtration chromatography, they were characterized using UV−vis spectroscopy, revealing a characteristic surface plasmon band at 522 nm. Their dispersity was confirmed by TEM (Figure 3, also see Supporting Information). The particles are extremely stable and can be centrifuged and resuspended several times without significant loss of

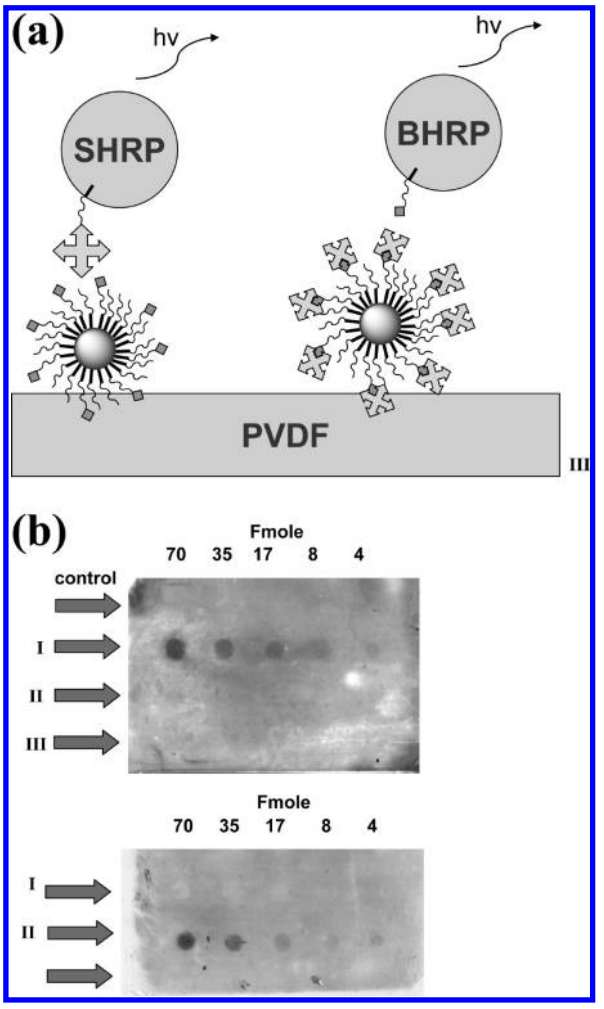

Figure 4. (a) Cartoon depicting dot-blot assay of 1%B−Au, SA-1%B−Au and L1-SA-1%B−Au: SHRP = StrepTactin horseradish peroxidase, BHRP = biotin horseradish peroxidase. (b) Dot-blot assay results. Dots probed with SHRP (top), dots probed with BHRP (bottom). Control = PEG−OH−Au, I = 1%B−Au, II = SA-1%B−Au, III = L1-SA-1%B−Au.

material. They are stable for up to 3 months when stored at 4 °C in deionized water and are compatible with biological buffers, tolerating salt concentrations up to 2 M before aggregation occurs. These properties are attributed to the structure of the alkylthiol-PEG ligands (Scheme 1), which contain a thiolate group for strong bonding to the gold nanoparticle surface and a water-soluble oligo(ethylene glycol) portion, which should also prevent denaturation of covalently bound proteins and reduce nonspecific binding to the particles.

Lipase−Nanoparticle Bionanoconjugate Formation. To link the biotinylated lipase to the biotinylated NPs, the well-known interaction between biotin and streptavidin has been exploited.[69] This method (Scheme 1) is based on the noncovalent but strong binding of up to four biotin molecules by streptavidin. In practice however, it has been observed that when streptavidin is used to bind bulky biotinylated objects, steric hindrance causes only two of the biotin-binding sites in streptavidin to be stably occupied.[70] By harnessing this strong binding interaction streptavidin may be used as a "glue" to link the biotinylated NP and lipases, as depicted in Scheme 1. To prepare the lipase−nanoparticle conjugates, the NPs are first "coated" with streptavidin. The excess of streptavidin has to be regulated so that we avoid cross-linking of the nanoparticles but at the same time not cause kinetic or thermodynamic instability of the colloids. After removal of excess streptavidin by repeated centrifugation and redispersion cycles, the particles (termed SA-x%B−Au, where x = the percentage of biotin ligands in the NP ligand shell) were mixed with a 20-fold molar excess of biotinylated lipase variant, incubated overnight, and finally purified by centrifugation and redispersion as before. To ensure complete removal of unbound lipase, the supernatant from each centrifugation cycle was tested for lipase activity, and the cycles repeated until no activity was detected in at least four consecutive washes (see Supporting Information). TEM (Figure 3) confirms that functionalizing the NPs with streptavidin and lipase does not cause them to aggregate significantly.

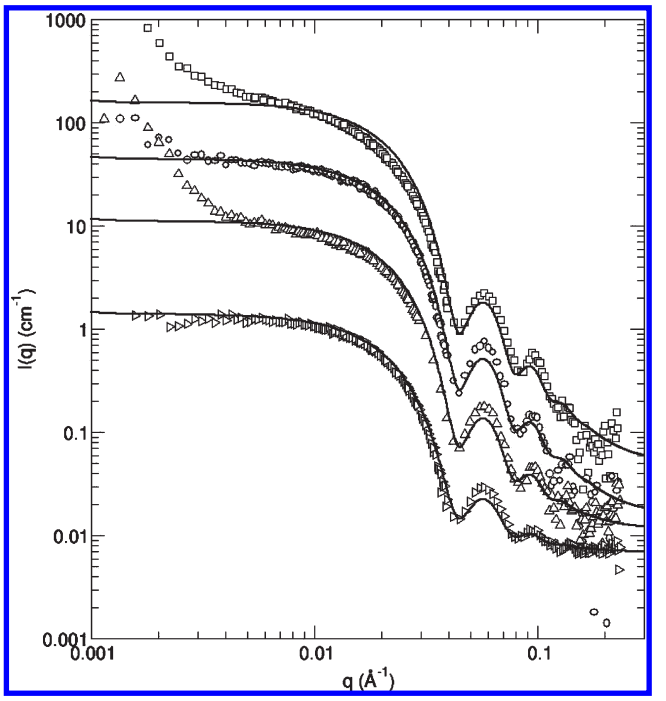

Figure 5. Scattered intensity for gold particles (0.2% by weight and for lipase-modified particles 0.02% by weight) coated step-by-step with $SC_{11}E_4$ in D_2O (squares), $SC_{11}E_4$ + $SC_{11}E_3$−biotin in D_2O (circles), $SC_{11}E_4$ + $SC_{11}E_3$−biotin + streptavidin D_2O (reversed triangles), and $SC_{11}E_4$+$SC_{11}E_3$−biotin+streptavidin+lipase in D_2O (triangles) as obtained by small-angle neutron scattering. The measurements were conducted at room temperature. The solid lines are fits to a smeared, polydisperse core−shell form factor, where the gold core has a radius of 7.5 nm and shell thickness of the layer is about 1.5 nm. Note that the same fit can be used for all cases as the density of the biotin is very low and the difference in scattering length density when binding a few enzyme molecules to the particle is not enough to detect changes.

Dot-blot tests were used to evaluate the specific binding properties of the conjugates. The scheme is illustrated in Figure 4a, where the NPs (dotted onto a porous membrane) were treated with either StrepTactin-horseradish peroxidase (to detect available biotin groups) or biotin-horseradish peroxidase (to detect available streptavidin groups). The dots were developed using a colorimetric substrate for the horseradish peroxidase and the results are presented in Figure 4b. The top image shows that biotin is only detected on 1%B−Au. The result for SA-1%B−Au and L1-SA-1%B−Au are the same as for the PEG−OH−Au

(69) Wilchek, M; Bayer, E. In *Methods in Enzymology*; Abelson, J. N., Wilchek, M., Simon, M. I., Bayer, E. A., Eds.; Academic Press: San Diego, 1990; Vol. *184*.
(70) Niemeyer, C. M.; Adler, M.; Pignataro, B.; Lenhert, S.; Gao, S.; Chi, L.; Fuchs, H.; Blohm, D. *Nucleic Acids Res.* **1999**, *27*, 4553–4561.

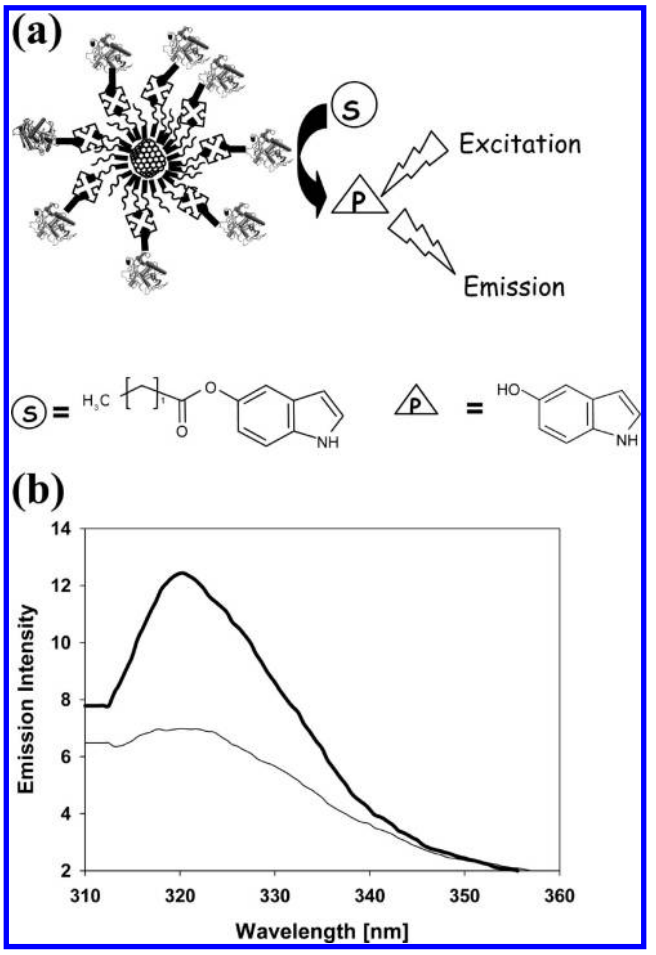

Figure 6. (a) Cartoon depicting lipase activity of lipase−AuNP bionanoconjugates and (b) fluorometric lipase assay emission spectra recorded after 1 min (thin line) and 5 min (thick line) of incubation with L1-SA-10%B−Au.

Table 1. Comparison of Lipase Activity Assay Results for All Lipase−Nanoparticle Bionanoconjugates

lipase	% biotin ligands per NP	activity per nM of NP conjugate[a,b]
L1	1%	0.091 ± 0.018
L2	1%	0.341 ± 0.027
L1	10%	0.223 ± 0.001
L2	10%	0.436 ± 0.072

[a] Concentration of NPs in the sample determined by UV−vis with $\varepsilon = 2.89 \times 10^8$ M^{-1} cm^{-1}. [b] Activity is expressed as U L^{-1}, where 1 U (unit) is the amount of enzyme which liberates 1 μmol of lipase assay product per min.

control sample, demonstrating the expected absence of accessible biotin groups; as in the NPs all the accessible biotin groups have been bound to streptavidin. The bottom image shows that streptavidin is detected only on SA-1%B−Au, with the expected absence of streptavidin on 1%B−Au. It also demonstrates that the streptavidin in the L1-SA-1%B−Au samples cannot be detected, indicating that the streptavidin is unaccessible, having been "used up" in binding the lipase to the NP; that is, the streptavidin layer has been "coated" with an outer layer of lipase. Biotin is also not detected in these samples. This provides further evidence for the successful conjugation of lipase to NP.

SANS Characterization of the Lipase−Nanoparticle Bionanoconjugates. To characterize complex core−shell type functionalized gold NPs and verify the low content of lipase molecules on the outermost layer, a SANS study was employed. The aim of the SANS study is the characterization of the increased complexity of the gold nanoparticles during the step-by-step functionalization (L2-SA-10%B−Au bionanoconjugates). To enhance the particle contrast and reduce incoherent scattering, experiments were performed in heavy-water-based buffer solutions.

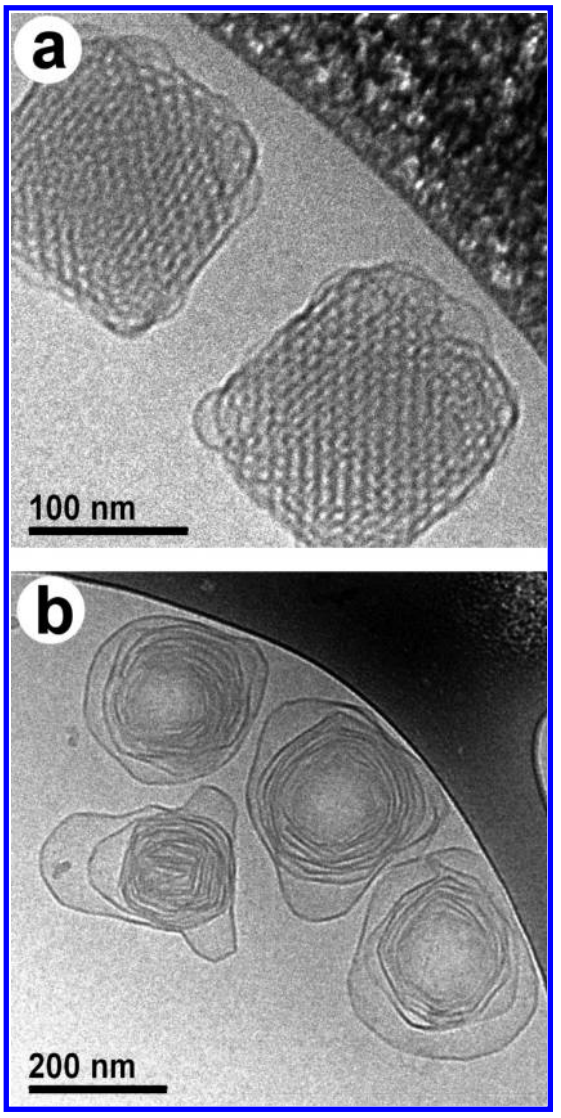

Figure 7. Representative cryo-TEM micrographs of (a) typical appearance of GMO-based nanostructured cubosomes viewed along the [100] direction and (b) cubosome transformation into onion-like multilamellar aggregates after exposure to wild-type lipase solution.

Figure 5 shows SANS intensities of NPs at different steps of functionalization where experimental data are fitted with a form factor for core−shell particles. The solid lines in Figure 5 represent the best fits which have been obtained using the same form factor parameters for all curves keeping ρ_{core} fixed to ρ_{Au} (4.00×10^{-4} nm^{-2}) and the solvent to ρ_{D_2O} (6.33×10^{-4} nm^{-2}) in agreement with core−shell particles with a polydispersity of 9%, core radius of 7.5 nm, and a shell thickness of 1.5 nm. The scattering length density of the shell was determined to 0.88×10^{-4} nm^{-2}, which suggests 12 vol % of D_2O present in the self-assembly layer using the literature value of $C_{12}E_5$ (0.133×10^{-4} nm^{-2}). The layer thickness is in agreement with SANS data for a droplet microemulsion consisting of $C_{12}E_5$. The upturn at low q in the scattering

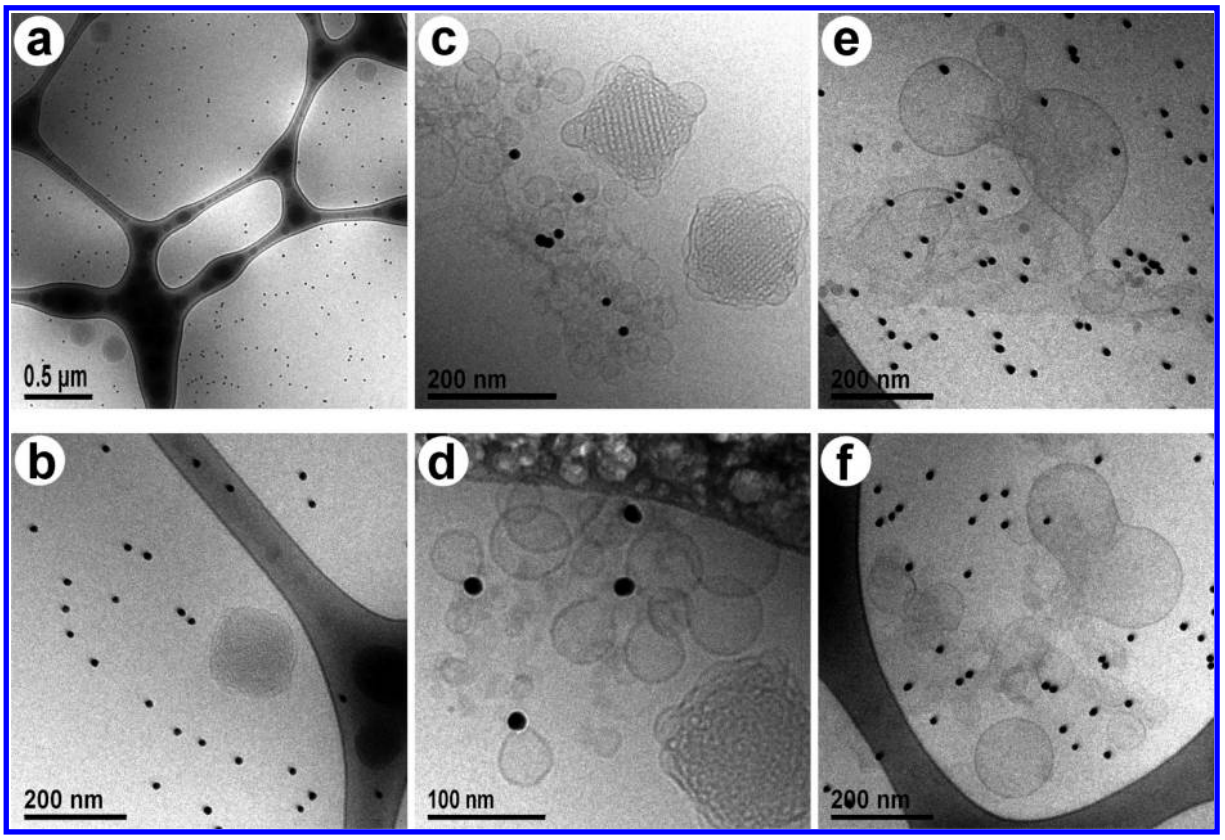

Figure 8. Representative cryo-TEM micrographs of intact GMO-based cubosomes in the presence of the streptavidin−gold nanoparticle bioconjugates (no lipase on the outermost gold nanoparticle layer) (a and b) and GMO hydrolysis induced transformation of cubosomes into unilamellar vesicular type aggregates after incubation with lipase functionalized gold nanoparticles (c−f).

curves most likely originate from the particle aggregates and is not taken into account in the fitting.[71] These results confirm the low density of streptavidin and lipase molecules on the particles as it comes from the low degree of biotinylation of the protective layer. Importantly, it shows the efficiency of the protective layer in preventing nonspecific protein interactions with the gold core. The measurements at theoretical contrast match point of gold (70% of heavy water) have also been done. Although the quality of the data due to the lower intensity and higher background scattering is not as good as for pure heavy water, the scattering curves can be also fitted with the same set of parameters.

Fluorescence-Based Lipase−Nanoparticle Bionanoconjugates Activity Assay. The lipase−NP conjugates were assayed for lipase activity using the same fluorometric lipase assay employed earlier for the characterization of free enzyme (schematically depicted in Figure 6a). Figure 6b shows the increase in emission from the assay product (5-OH-indole) recorded after 1 and 5 min incubation with the lipase−NP conjugates. Table 1 summarizes the lipase assay results (in activity units, U L^{-1}, see Materials and Methods for definition) for all lipase−NP conjugates. Comparing rows 1 and 2 and rows 3 and 4 in Table 1 demonstrates that for both lipase variants, the measured activity is higher for the 10%B−Au lipase conjugates than for the 1% B−Au conjugates, but there is less than the 10-fold difference that may be predicted simply on the basis of the numbers of biotin groups on the NP surface. This suggests that the limiting factor in binding large numbers of lipase to NP may not be the availability of biotin-binding sites on the NP, but rather steric effects relating to the hydrodynamic size of the materials. The most interesting observation from Table 1 is the activity difference between the conjugates of L1 and L2. Comparing rows 1 and 3 and rows 2 and 4 in Table 1 indicates that regardless of whether 1%B−Au or 10% B−Au is utilized, the measured activity is consistently higher for L2 (3.8 fold higher for 1%B−Au and 2.2 fold higher for 10% B−Au). Recall from Figure 1 that the biotin label on L2 is located in a position opposite to the enzyme lid and active site, in contrast to L1, where the label is located adjacent to the active site. The results therefore indicate that binding the lipase to the nanoparticle using L2's binding site is more favorable for retaining enzyme activity, which is consistent with a model where, depending on the orientation of the enzyme, access to the active site can be blocked by the nanoparticle.

Wild-Type Lipase Activity on GMO-Based Cubosomes. Figure 7a shows the typical appearance of cubically shaped GMO-based cubosomes viewed along the [100] direction. The overall dispersion is homogeneous with a mean particle size of about 200 nm and an internal structure consistent with the body centered cubic Q^{229} of the $Im\bar{3}m$ space group. As evidenced from Figure 7b, the morphology of the lipid particles becomes dramatically different upon exposure to wild-type lipase solution. Initially well-structured cubic particles undergo transformation into onion-like lamellar aggregates. Naturally, the lipase hydrolyzes the esteric bond of GMO, with the concomitant formation of oleic acid and glycerol. It is therefore suggested that the formation and accumulation of oleic acid within the lipid particle during lipolytic reaction is responsible for this dramatic structural change. Recent phase behavior and aggregate structure studies of mixtures of GMO and oleic acid support this suggestion. It has been demonstrated that the addition of oleic acid promotes the

(71) Bagger-Jörgensen, H.; Olsson, U.; Mortensen, K. *Langmuir* **1997**, *13*, 1413–1421.

formation of lamellar-type aggregates at pH values higher than 8 where the fatty acid is mostly ionized.[72]

Lipase−Nanoparticle Bionanoconjugates Activity on GMO-Based Cubosomes. The effect of synthetic lipase−NP conjugates (L2-SA-10%B−Au bionanoconjugates) on cubosome dispersion is shown in Figure 8. From several hundred analyzed cryo-TEM micrographs it may be concluded that streptavidin-coated nanoparticles (no lipase on the outermost layer) have no effect on the morphology of the lipid particles. This is illustrated in Figure 8a,b where the cubosomes remain unchanged in the presence of the streptavidin−gold nanoparticle bioconjugates. In contrast, the images presented in Figure 8c−f clearly demonstrate the hydrolysis of cubosomes by lipase-functionalized gold nanoparticles. The resulting localized vesicular structures in close proximity to the gold nanoparticles undoubtedly demonstrate the enzymatic action. Localized pools consisting of tens of vesicles and various intermediate bilayer fragments are the remainder of the initially nanostructured GMO-based cubic particles. The use of lipase bound to gold nanoparticles leads to the formation of discrete vesicular structures, but not onion-like structures as in the case when the wild-type lipase solution is used. It is likely that the free enzyme molecules are capable of penetrating the porous bicontinuous lipid particles (the pore sizes are close to 10 nm and are slightly larger than enzyme dimensions) and acting to hydrolyze them from both outside and inside, leading to the formation of onion-type bilayers. In contrast, lipase−gold nanoparticle bioconjugates may simply be too large to penetrate the lipid particles, and therefore most of the enzymatic action occurs at the surface, facilitating the formation of discrete unilamellar vesicles. Furthermore, as each gold nanoparticle carries roughly from 1 to 4 lipase molecules, the local enzymatic activity is much higher when compared to a homogeneously distributed solution of enzymes. We have previously demonstrated the attachment of lipase to gold nanoparticles via click chemistry,[63] which can be used as an alternative albeit comparatively more cumbersome functionalization strategy. Preliminary cryo-TEM data obtained with such particles gave comparable results.

(72) Ferreira, D. A.; Bentley, M. V. L. B.; Karlsson, G.; Edwards, K. *Int. J. Pharm.* **2006**, *310*, 203–212.

Conclusions

A biotin−streptavidin linking strategy has successfully been employed to create lipase−gold conjugates with two different orientations of the enzyme. Lipase variants with biotin labels incorporated at different sites on the protein's outer surface have been used to control the orientation of the enzyme. Enzymatic activity appears to be orientation dependent with a significant decrease if the active site is facing the nanoparticle. The system represents a simple example of how the activity of a biomolecule can be controlled by binding it to a nanoparticle of similar size. In this case the relevant control parameter is the orientation of the biomolecule relative to the adjacent nanoparticle. There are many other factors such as charge, surface catalytic activity, shape, and chemical functionality of the nanoparticle that could be used to couple to biomolecular activity and hence there is an opportunity to produce a new range of bionanomaterials with enhanced functionality. The biotin/streptavidin linking method appears to be a straightforward and fairly general strategy for the creation of such hybrids. It has been shown that conjugation of lipase to metal nanoparticles results in enzymatically active hybrid nanoparticles, which were used to visualize the enzymatic digestion of lipid aggregates. Notably, the use of lipase−gold nanoparticle conjugates instead of lipase alone affects the manner in which enzymatic digestion occurs at the single molecule level which opens up new possibilities to provide a handle on single lipase molecules.

Acknowledgment. This work was supported by the EU-STREP FP6 project BIOSCOPE (Contract No. NMP4-CT-2003-505211) and Project AuTEK. We are grateful to Gunnel Karlsson (Lund University, Sweden) for assistance with the cryo-TEM instrumentation, Martin C. Feiters (Radboud University, Netherlands) for assistance with initial SANS experiments, Dr. Laurence Duschene for help with the dot-blot assay, and Stephen Apter for elemental analysis.

Supporting Information Available: Tables of lipase activities of supernatants from nanoparticle washing steps and agarose gels of lipase−nanoparticle conjugates. This material is available free of charge via the Internet at http://pubs.acs.org.